ISSN 0915-633X

NATIONAL INSTITUTE FOR FUSION SCIENCE

Alfven Instabilities in FRC Plasma

Andrey N. Lyakhov

(Received - Nov. 25, 1997)

NIFS-526 Dec. 1997

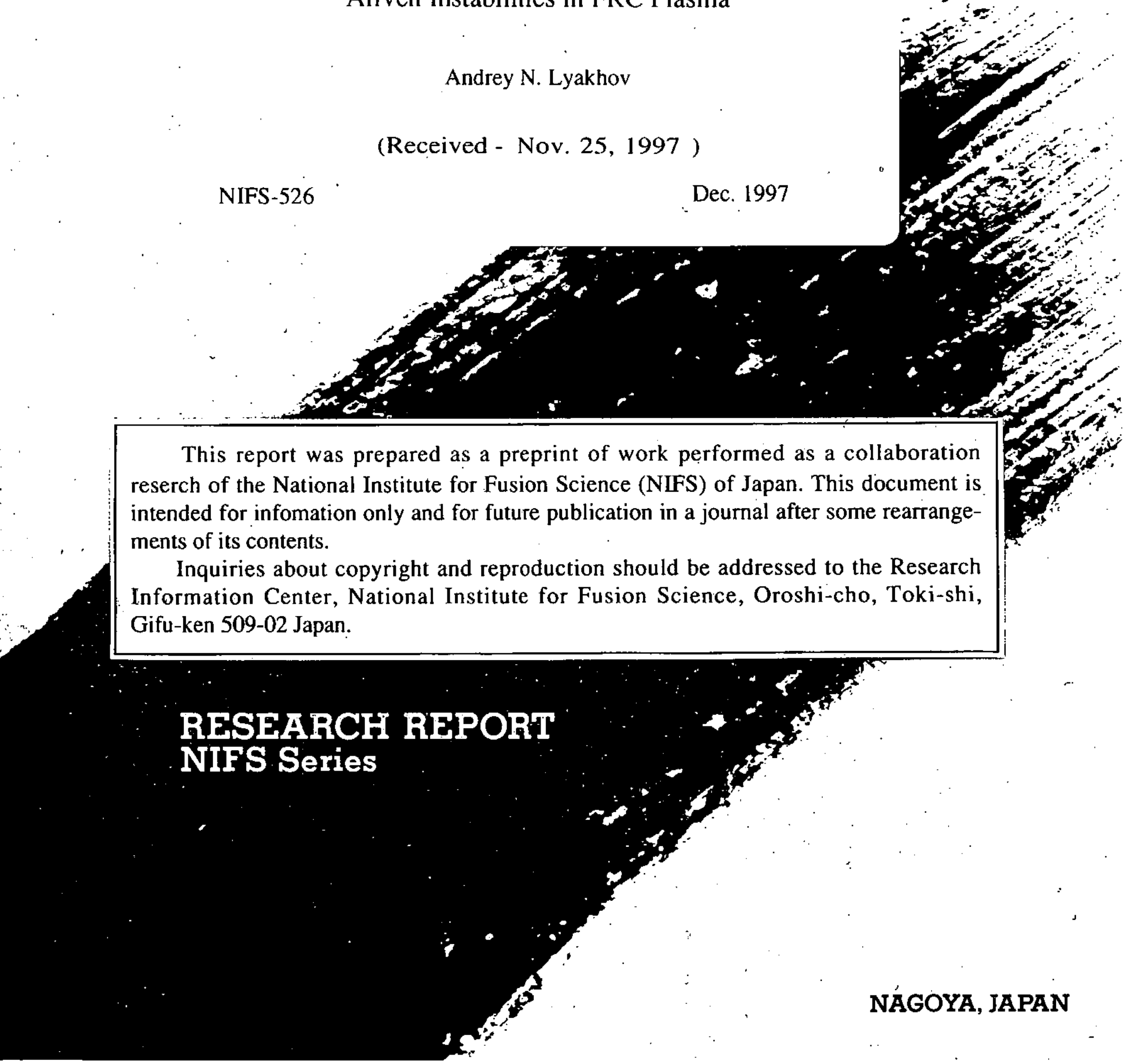

RESEARCH REPORT
NIFS Series

NAGOYA, JAPAN

Alfven instabilities in FRC plasma

Andrey N.Lyakhov[*]

National Institute for Fusion

Science, Toki-shi, Gifu 509-52 Japan

Abstract

The stability of Alfven-type waves in a Field-Reversed Configuration was studied and preliminary results are presented. Predicted frequency range is found to be in a good agreement with the experimental data. Saturation model has been developed in the framework of nonlinear wave-particle resonant model. The comparison of calculated saturation time and fluctuation level with experiment is presented. The model of anomalous transport is discussed.

Keywords:FRC,Stability,Alfven,Anomalous Transport,FIX

---

[*] On leave from Bauman Moscow State Technical University,Moscow 107005,P.O.Box 38, Russia

I. INTRODUCTION

For the long time the problem of transport processes in a Field Reversed Configuration exist. Experimental data give reasons to consider particle transport in FRC as anomalous [1]. As one of the reasonable source microinstabilities can be considered. So it is necessary to find out, what instability really exist in FRC plasma.

Previously the main attention has been paid to drift-dissipative instabilities [2], [3] . But the experiments on TRX installation have shown no presence of LHD activity [4]. In later experiments on FIX installation on the measurement of magnetic field fluctuation spectra have been obtained that are also unidentified [5].

The following properties of FRC are most important for the stability analysis:high plasma beta, nonuniform pressure and nonuniform magnetic field. The previous analysis consider mainly potential microinstabilities caused by pressure gradient. Effects of high beta have been taken into account, but the final result has not depended on magnetic field nonuniformity.

Here we consider electromagnetic instability of Alfven-type wave in plasma with all nonuniformities taken into account, and the fact that local $\beta \to \infty$ together with FLR effects is described correctly.

In section II we briefly describe the assumptions and the mathematical model of FRC plasma. In section III results on linear stage of instability are presented. Section IV describes the nonlinear saturation model. In section V we discuss the results on nonlinear model and compare them with the experiments.

II. MATHEMATICAL MODEL

We consider FRC in the slab geometry approximation, Magnetic field is taken in the form of Hill's vortex configuration

$$\Psi(r, z) = \frac{B_0 r^2}{2}\left(1 - \frac{r^2}{a^2} - \frac{z^2}{b^2}\right) \tag{1}$$

Here a-separatrix radius, $a/b = \epsilon$ - elongation of magnetic field. In our analysis we neglect z-dependencies, so considering only middle-section. This assumption well describes the highly elongated FRC, which is of interest for reactor prospects [6]. So below we will replace r by x dependence. Magnetic field profile is shown in Fig.1.

Pressure profile was taken in the form (Fig.2):

$$p(x) = p_0 exp\left(-K_n \frac{x^2}{a^2}\right) \tag{2}$$

which coincides well with the experimental data [5], if the shape factor $K_n \simeq 3$. Then the local β value is $\beta(x) = 8\pi p(x)/B^2(x)$ and is shown on Fig.3.

In a high beta plasma the perturbations with long wavelength's are described by the following dispersion relation (in a zero gyroradius approximation) [7] in the local approximation, so with all paramters depend on x coordinate, and assuming that distribution function is Maxwellian:

$$Q = \left(\frac{c^2}{c_A^2}\right)\left(\omega^2 - \omega\Omega_i - n\omega_{Bi}\Omega_i - k_z^2 c_A^2\right) = 0 \tag{3}$$

where c_a - Alfven velocity, c - speed of light, ω- mode frequency,k_z - parallel wave vector, Ω_i - drift frequency on magnetic field gradient:

$$\Omega_i = \frac{\kappa_b k_\perp T_i}{m_i \omega_{Bi}} \tag{4}$$

where $\omega_{Bi} = (eB)/(m_i c)$ - ion gyrofrequency, T_i, m_i - ion temperature and mass, and κ_b (relative gradient) is defined as follows:

$$\kappa_b = \frac{dlnB}{dx} = \frac{1}{B}\frac{dB}{dx} \tag{5}$$

together with the relative density gradient

$$\kappa_n = \frac{dlnN}{dx} \tag{6}$$

This dispersion equation has the analog in the case of spatially uniform plasma, which describes Alfven waves. In the nonuniform plasma it is impossible to select different waves in the same manner, so we will simply call the waves, described by (3) as the Alfven-type waves.

Eq.(3) has two solutions:

$$\omega_1 = \Omega_i \tag{7}$$

$$\omega_2 = -n\omega_{Bi} - \frac{k_z^2 c_A^2}{\Omega_i} \tag{8}$$

To study the process of wave growth it is necessary to add to (3) FLR term Q_1 [7].

$$ImQ_1 = \frac{c^2}{c_a^2}\frac{9}{8\sqrt{\pi}}(k_\perp \rho_i)^2 |k_z| v_{Ti} \frac{(1+\omega_n/\omega)^2}{(1+\omega_n/2\omega)} \tag{9}$$

where $\omega_n = n\omega_{Bi}$ and ω is to be replaced by the solutions of (3) from (7),(8).

The dimensionless wave energy is given by

$$W = \frac{1}{\omega}\frac{dQ}{d\omega} \tag{10}$$

and the dissipation is $\Xi = \omega ImQ_1$

Energy of Alfven-type waves from (3) is $W \sim (2 - \Omega_i/\omega)$ and it is negative if $\Omega_i > 2\omega$. This condition is fulfilled with the root ω_2. Such perturbations will be unstable in the case of positive dissipation $\Xi > 0$. The last condition is fulfilled for ω_2, so the waves with negative energy will be unstable. Energy of Alfven-type waves is negative in the case, when

$$\xi_{bn} = \frac{\kappa_b}{\kappa_n} < 0 \tag{11}$$

and this means the region, where ∇B and ∇N have different signs. According to Fig.1,2 one can see that condition (11) is fulfilled in the outer region of FRC.

For such unstable waves the growth rate is given by

$$\gamma = -\frac{ImQ_1}{\partial Q/\partial\omega} \tag{12}$$

And for the case (8) the growth rate is

$$\gamma = \frac{9}{8\sqrt{\pi}}(k_\perp \rho_i)^2 |k_z| v_{Ti} \frac{(1-\omega_{ni}/|\omega_2|)^2}{1-\omega_{ni}/2|\omega_2|} \frac{1}{\Omega_i + 2\omega_{ni} + 2k_z^2 c_A^2/\Omega_i} \tag{13}$$

Growth rate (13) reaches its maximal value at

$$k_z = \sqrt{|\xi_{bn}|}\frac{\omega_{ni}}{c_A} \tag{14}$$

where $\omega_{ni} = n\omega_{Bi}$.

III. RESULTS

Below we present the results of calculation of frequency, wavelengths and growth rates for the FRC plasma. In order to compare these results with the experiment, we choose all plasma parameters as in the FIX experiment [5].

Separatrix radius, $a = 40cm$; plasma density $n_0 = 5 \cdot 10^{13} cm^{-3}$; and plasma temperature $T_i = T_e = 150eV$. The results are as follows.

Wavelengths slightly vary with radius, from 0.42 cm^{-1} to 0.33 cm^{-1}.

Normalized growth rate of Alfven-type instability is presented in Fig.4. The region left to $\simeq 0.87a$ is out of analysis, because there $\gamma > \omega$. In the outer region of FRC typical growth rates vary from $\simeq \omega_{Bi}$ to $0.05\omega_{Bi}$ at the separatrix. Such large values gives us the reason to consider Alfven-type waves instability as a real candidate on the role of the source of anomalous losses.

Wave frequency is presented in Fig.5 and Fig.6. In Fig.5 frequency is normalized to ion gyrofrequency, and in Fig.6 to the low-hybrid frequency. In the region of unstable waves (Fig.4) Alfven-type waves have frequency from $1.1\omega_{Bi}$ to $1.1\Omega_{LH}$ at the separatrix.

In the experiments on the measurement of magnetic field fluctuations in a field reversed configuration plasma, fluctuations were observed at the frequency range $3\omega_{Bi} - 0.4\Omega_{LH}$. Relative amplitudes were about $\tilde{B}/B \sim 1 - 1 \cdot 10^{-4}$. We shall compare the last result with theory in section IV. And here in conclusion we want to mention the fact, that Alfven type instability has the frequencies which lay in the observed region. The fact, that predicted frequency near the separatrix is slightly higher than the observed one $1.1\Omega_{LH}$ instead of $0.4\Omega_{LH}$ can not be considered as an argument against Alfven waves. In FIX machine elongation $\epsilon \simeq 5$, so this can be explained by

1)slab model is not enough near the sepratrix, where the effects caused by the curvature of a magnetic field force line may play the significant role;

2) the plasma profiles used in calculation save the qualitative features of realistic data, but exact results may differ (in any case in less than an order).

So we see that the analysis of Alfven-type waves in FRC leads to the results which coincide well with the known experimental data. High growth rates allows to consider Alfven type instability as a serious fact in the picture of anomalous transport.

IV. NONLINEAR SATURATION MODEL

We proceed with one particle Hamiltonian

$$H = \frac{1}{2m_i}\left(\vec{p} - \frac{e}{c}\vec{A}\right)^2 - \frac{e}{c}\vec{v}\vec{A}_1 \tag{15}$$

where $\vec{A}_1$ - perturbed part of vector-potential $\vec{B} = \nabla \times \vec{A}$, which appears due to the Alfven-type wave. Assuming the action variables as

$$\begin{pmatrix} J_g \\ P_y \\ p_z \end{pmatrix} = \begin{pmatrix} \frac{mv_\perp^2}{2\omega_{Bi}} \\ mv_y + \frac{e}{c}A \\ mv_z \end{pmatrix} \tag{16}$$

and determining conjugate angles as θ_q - gyrophase, Y- y-coordinate of guiding center,z -coordinate of the particle, and noting that P_y - is the constant of motion we rewrite Hamiltonian in the form:

$$H = \frac{p_z^2}{2m} + \omega_{Bi}J_g - \frac{e}{c}v_z A_1 \sin(k_z z + k_\perp y - \omega t) =$$

$$= \frac{p_z^2}{2m} + \omega_{Bi}J_g - \frac{e}{c}v_z A_1 \sin(k_z z + k_\perp \rho \sin(\varphi) - \omega t) = \tag{17}$$

$$= \frac{p_z^2}{2m} + \omega_{Bi}J_g - \frac{e}{c}v_z \tilde{A}_1 \sum_l \Im_l(k_\perp \rho) \sin(k_z z + l\phi - \omega t)$$

Here we expand the assumed form of the perturbation into the series in ordinal Bessel functions $\Im_l\,(k_\perp \rho)$ of order l.

Redefining $\vec{J} = (J_1, J_2) = (p_z, J_g)$ and $\vec{\theta} = (\theta_1, \theta_2) = (z, \phi)$ we rewrite(17) in the more convenient form:

$$H = H_0(\vec{J}) + V(\vec{J}, \vec{\theta}, t)$$

$$H_0(\vec{J}) = \frac{1}{2m}J_1^2 + \omega_{Bi}J_2 \tag{18}$$

$$V(\vec{J}, \vec{\theta}, t) = -\frac{e}{mc}\tilde{A}_1 J_1 \sum_l \Im_l(k_\perp \rho) \sin(k_z \theta_1 + l\theta_2 - \omega t)$$

This is the non-canonical case in the framework of nonlinear physics. It is very interesting, that in the well known studying of wave-particle interaction in the case of electrostatic instabilities perturbation in (18) does not depend on action variables, which fact, in turn, allows to reduce the whole problem to standard - mapping technique and obtain diffusion coefficients in easy way. Here the perturbation depends on action variable. So strictly speaking, it is necessary to use Li transforms, going to the action variables of the next order [8]. Below we will stay in the local approximation.

So using standard methods we eliminate all harmonics except l and enter new phase $\xi = k_z\theta_1 + l\theta_2 - \omega t$. Then $V = V_{0l}J_1\sin(\xi)$, where amplitude

$$V_{0l} = -(e/mc)\tilde{A}_1\Im_l(k_\perp\rho) \tag{19}$$

So the local Hamiltonian is $H = H_0(J) + V_{0l}J_1\sin(\xi)$.

The resonant condition is as usual:

$$k_z v_z + l\omega_{Bi} - \omega = 0 \tag{20}$$

And it depends on radial coordinate. Then, choosing any set of resonant values k_z^0, l^0 we write equations of motion:

$$\begin{cases} \dot{J_1} = -V_{0l}J_1k_z^0\cos(\xi) \\ \dot{J_2} = -V_{0l}J_1l\cos(\xi) \\ \dot{\theta_1} = \frac{J_1}{m} + V_{0l}\sin(\xi) \\ \dot{\theta_2} = \omega_{Bi} \end{cases} \tag{21}$$

Then we take the values at the resonance $J_1 = J_{10}, J_2 = J_{20}$, expand $H(J)$ in series on $(J_i - J_{i0})$ and take V at the point J_{i0}, thus obtain:

$$\begin{cases} \Delta\dot{J_1} = -V_{0l}J_{10}k_z^0\cos(\xi) \\ \Delta\dot{J_2} = -V_{0l}J_{10}l\cos(\xi) \\ \dot{\theta_1} = \frac{J_{10}}{m} + V_{0l}\sin(\xi) \\ \dot{\theta_2} = \omega_{Bi} \end{cases} \tag{22}$$

From resonance condition $v_z^0 = \frac{(\omega - l\omega_{Bi})}{k_z^0}$ and $J_{10} = (m/k_z^0)\,(\omega - l\omega_{Bi})$. So phase dynamics from (18) is:

$$\ddot{\xi} + k_z^0 V_{0l}\left(\omega - l\omega_{Bi}\right)\cos\left(\xi\right) = 0 \tag{23}$$

which is simply the equation of nonlinear pendulum with the frequency:

$$\Omega_s^2 = k_z^0\frac{e}{mc}\left(l\omega_{Bi} - \omega\right)\tilde{A}_1\Im_l\left(k_\perp\rho\right)\Big) \tag{24}$$

Then fixing any two neighboring resonances l and $l+1$ the distance between them will be $\omega_{B\imath}$. And the overlapping criteria is

$$K = \left(\frac{\Omega_s}{\omega_{B\imath}}\right)^2 \geq 1 \tag{25}$$

We suppose that the amplitude of the unstable wave will grow until the saturation. Under the saturation here we mean the fulfillment of the condition $K = 4.5$ which corresponds to the global stochastisation and destruction of resonant structure. Substituting expression for Ω_s to (25) we have

$$K(x,t) = k_z^0(x)\frac{e}{mc}\Im_l\left(k_\perp \rho\left(x\right)\right)\frac{l\omega_{B\imath}(x) - \omega(x)}{\omega_{B\imath}^2(x)}\tilde{A_{10}}e^{\gamma(x)t} \tag{26}$$

where the $\tilde{A_{10}}$ - thermal fluctuation level.

So the condition (25) will be realized in time from the central region to separatrix, and this can be considered as the movement of the front of saturation to the plasma border.

Inverting (26) it is easy to obtain expression for the saturation time, which will define the level of amplitudes of the perturbation.

$$\tau_s(x,l) = \left(\frac{1}{\gamma}\right)\ln\left(\frac{4.5}{k_z(x,l)\frac{e}{mc}\Im_l(k_\perp\rho(x))\tilde{A_{10}}|\frac{l\omega_{B\imath}(x)-\omega(x,l)}{\omega_{B\imath}^2(x)}|}\right) \tag{27}$$

V. RESULTS ON NONLINEAR SATURATION MODEL

In Fig.7 the results are presented on the calculation of overlapping time for FIX case. The front of saturation (or global stochastisation) moves outwards, to the separatrix. In Fig.8. the results are presented on the calculated relative amplitudes of magnetic field fluctuations, caused by Alfven instability. The calculated level has been defined as

$$B_f = B_f^{(0)}\exp\left(\gamma\tau_s\right) \tag{28}$$

where τ_s is defined in (27).

If we will take into account the Cherenkov damping of Alfven waves in this frequency region this will slightly change the growth rates near the separatrix, and will not cause sufficient changes in saturation time and in fluctuation level, because original growth rates are very large.

This calculated fluctuation level coincides in the order of magnitude with the experimental upper boundary of the amplitudes of oscillations of magnetic field. This fact could be explained by the disadvantages of the slab model together with the crudeness of nonlinear analysis which is to play more qualitative than quantitative role.

In conclusion we want again to mark especially the fact, that such type of instability is a kind of inherent property of an inhomogeneous plasma with high β. Another arguments for this instability as a realistic source of anomalous transport are that the correct analysis of drift waves of electrostatic nature shows, that the conditions of instability change significantly [9] and so such instabilities may not occur. Some results on such analysis in FRC case will be published elsewhere.

REFERENCES

[1] M. Tuszewski, Nuclear Fusion **28**, 2033(1988).

[2] N. Krall, Phys.Fluids **B 1**, 1811(1989).

[3] R.C. Davidson, Phys.Fluids **20**, 301(1977).

[4] A. Carson, Phys.Fluids **30**, 1497(1987).

[5] S. Okada, S. Ueki, H. Himura, S. Goto, Trans. of Fusion Technology **27**, 341(1995).

[6] H. Momota, A. Ishida, G.H.Miley, S. Ohi, M. Onishi, K. Sato, L. Steinhauer, Y. Tomita, M. Tuszewski, Fusion Technology **21**, 2307(1992).

[7] A.B.Mikhailovskii, *Electromagnetic Instabilities in an Inhomogeneous Plasma.* (Institute of Physics Publishing,Bristol,1992).

[8] A. Lieberman, A. Lichtenberg, *Regular and stochastic motion.* (Springer-Verlag, 1983).

[9] V.S. Beskin, A.V. Gurevich, Ya. I. Istomin, Sov.Phys. JETP **65**, 715(1987).

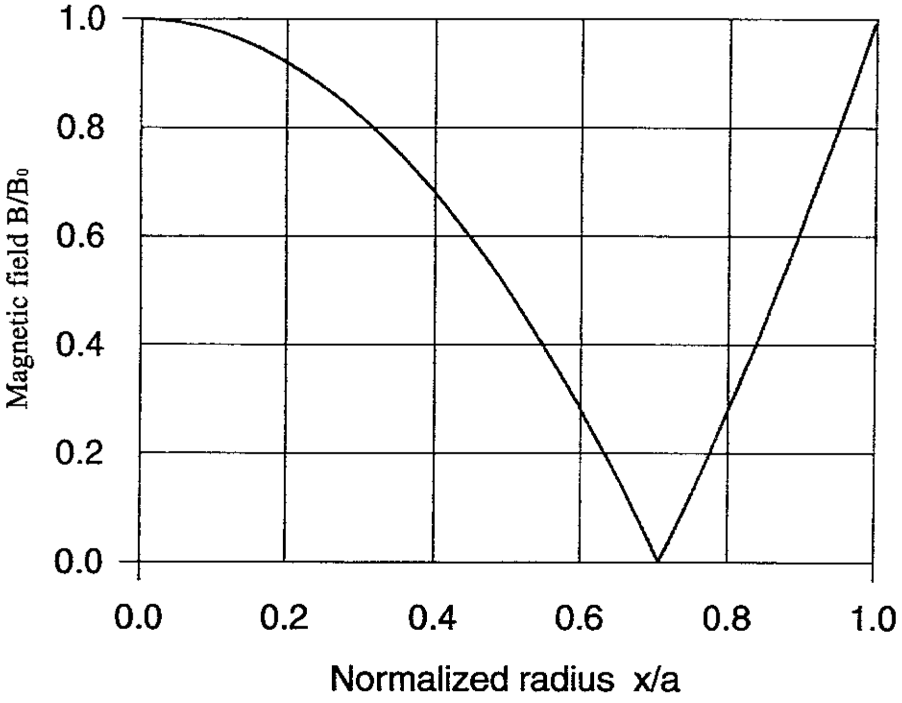

Fig.1. Magnetic field profile in a Field Reversed Configuration

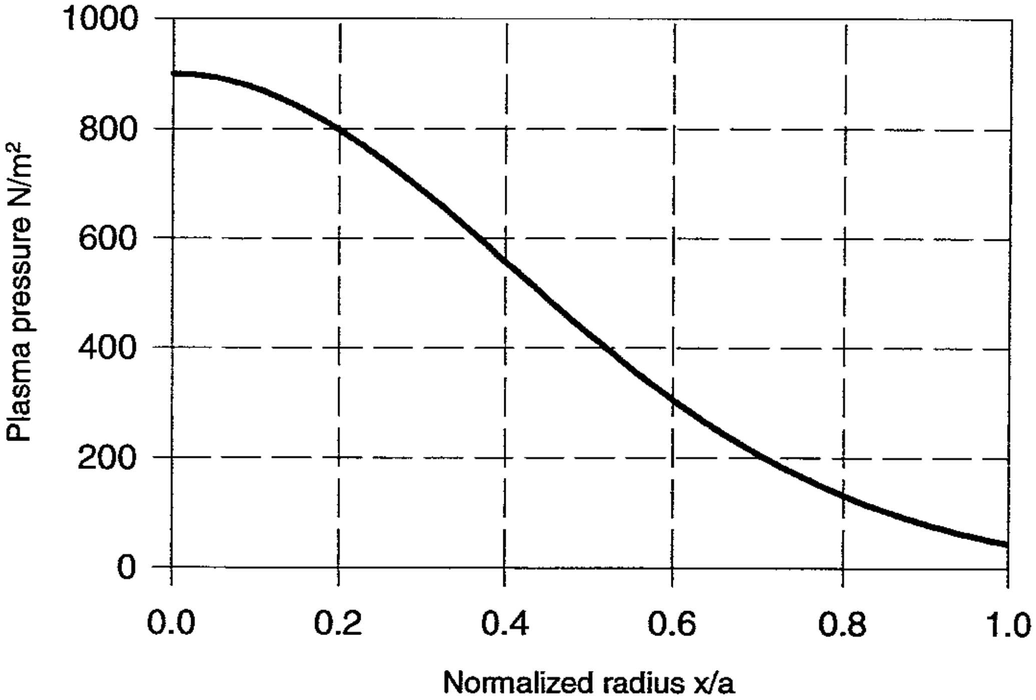

Fig.2. Plasma pressure profile in field reversed configuration

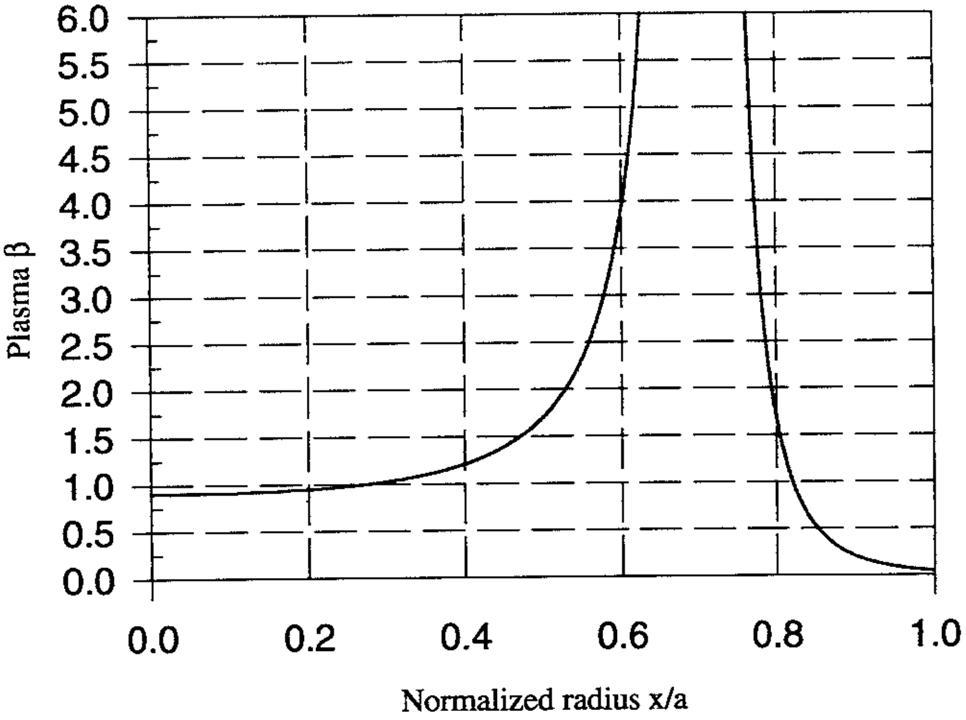

Fig.3. Plasma β value profile. Near the zero field region β tends to infinity.

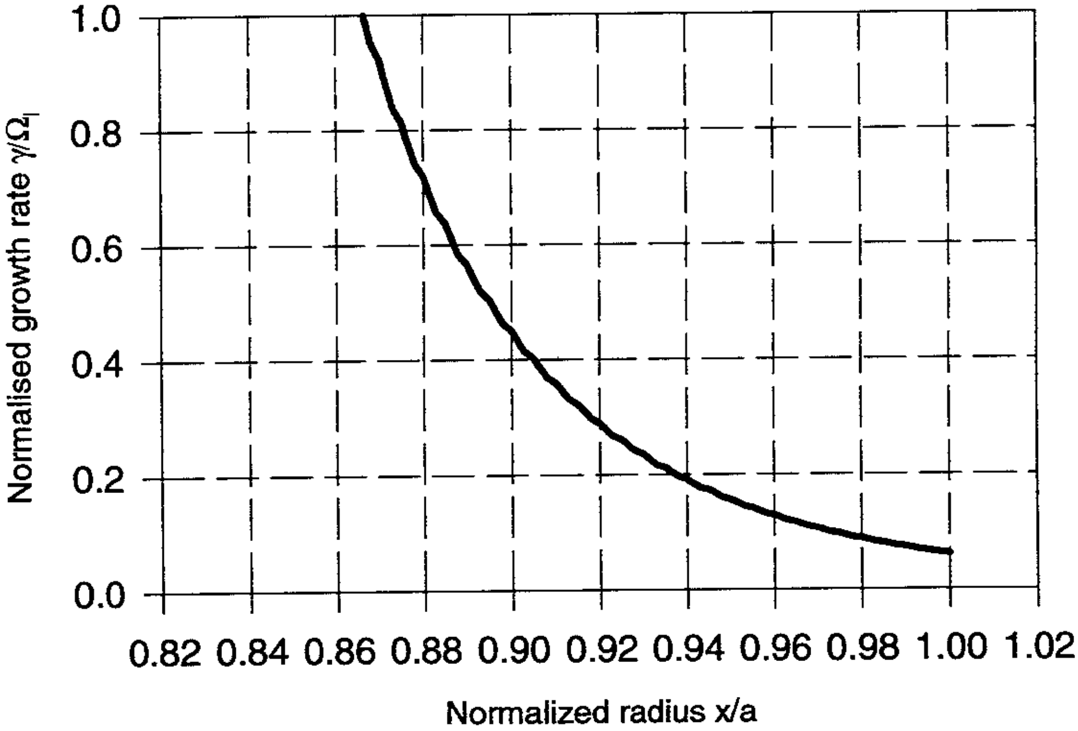

Fig.4. Normalized growth rate of Alfven instability

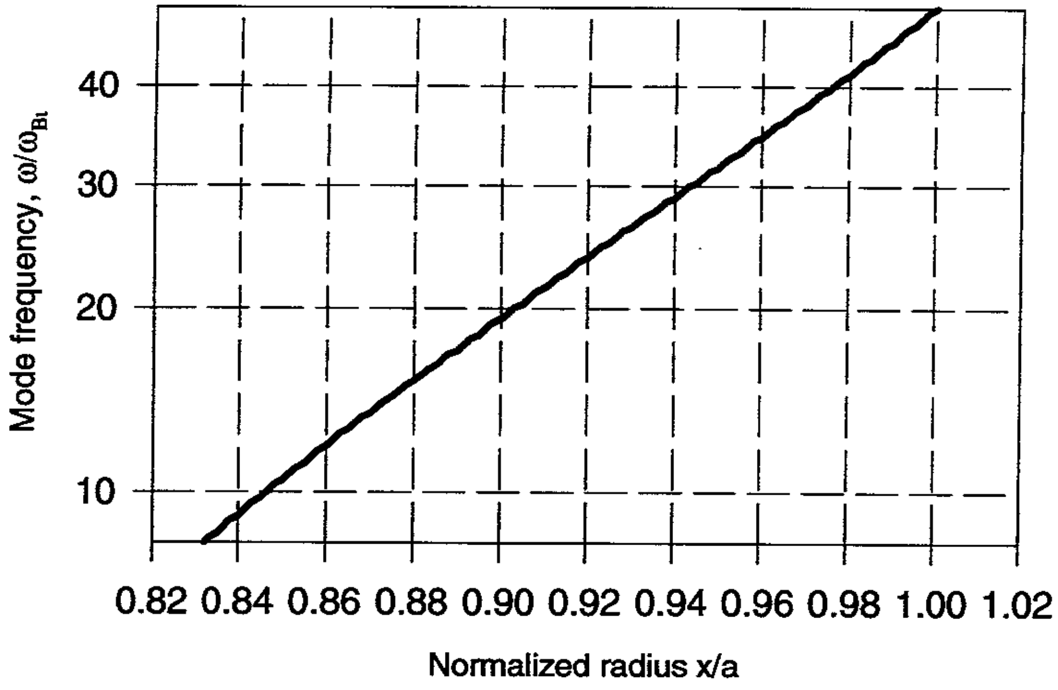

Fig.5. Mode frequency normalized to ion gyrofrequency

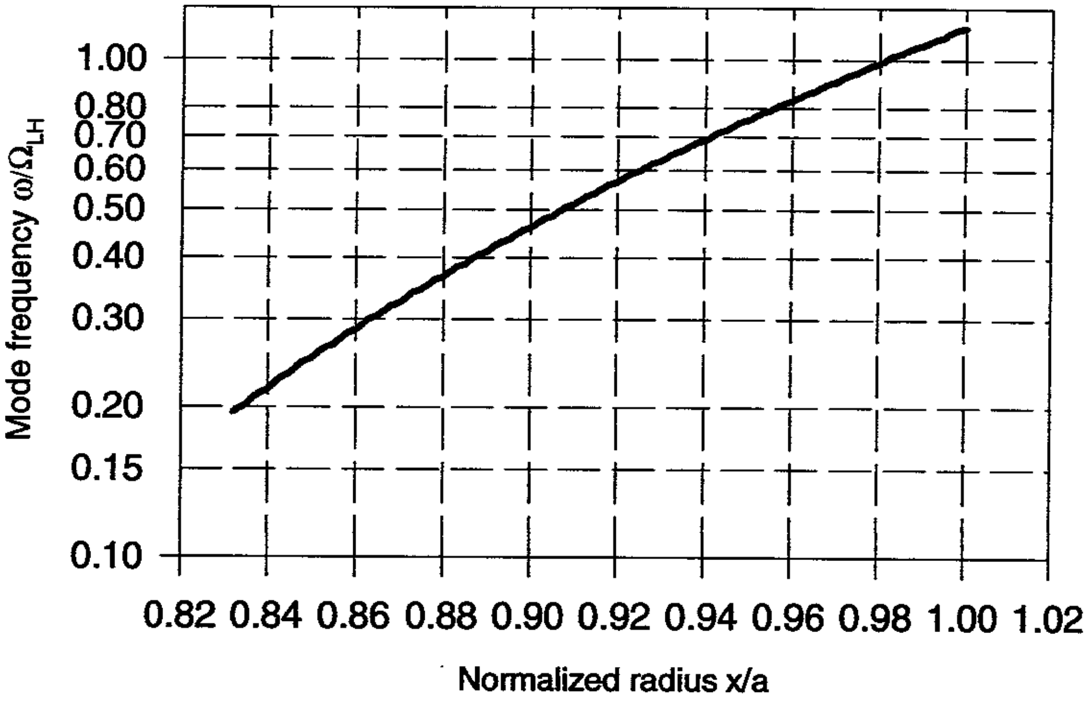

Fig.6. Mode frequency normalized to the low-hybrid frequency.

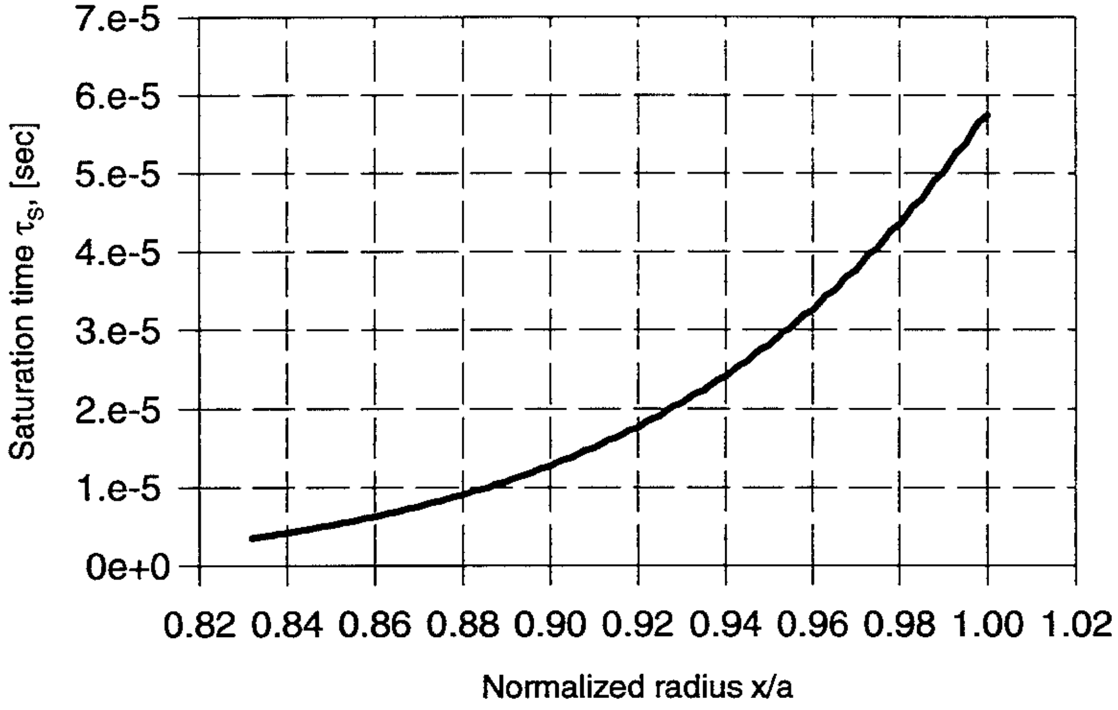

Fig.7. Saturation time τ_S - the time of global stochastisation.

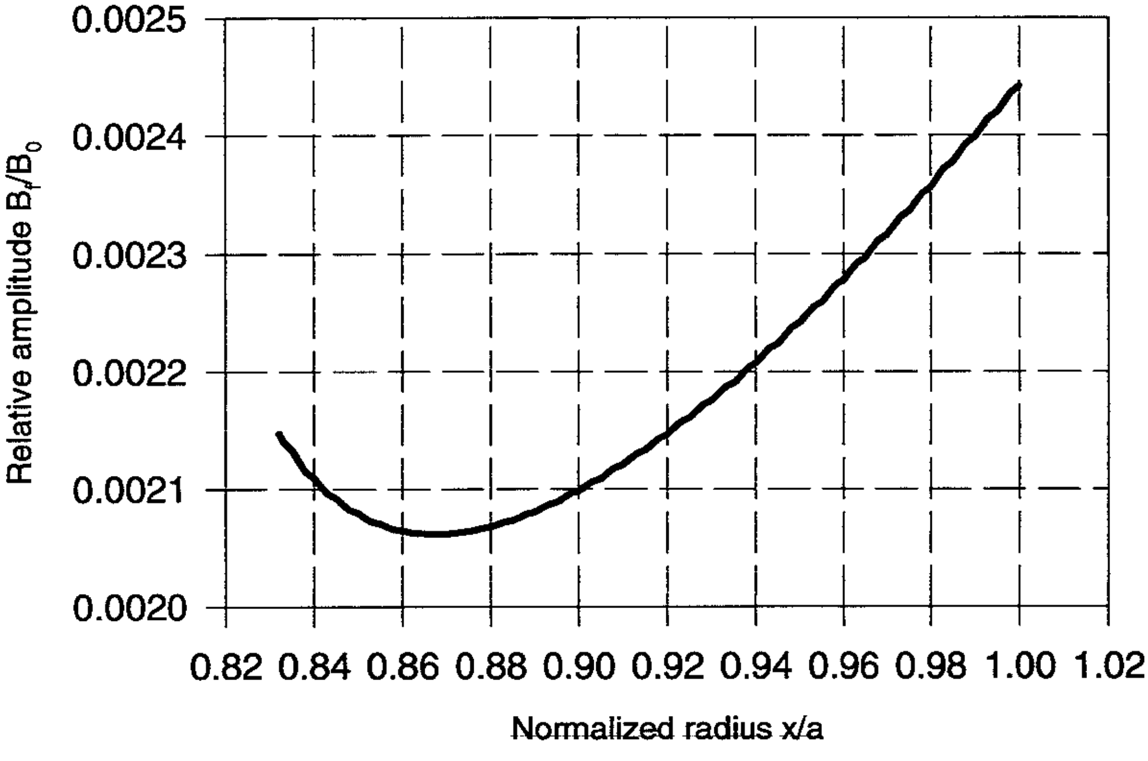

Fig.8. Fluctuation level at the saturated state.

Recent Issues of NIFS Series

NIFS-477	H. Kuramoto, K. Toi. N. Haraki, K. Sato, J Xu, A. Ejiri, K. Narihara. T. Seki, S. Ohdachi, K. Adati, R. Akiyama, Y. Hamada, S. Hirokura, K. Kawahata and M. Kojima, *Study of Toroidal Current Penetration during Current Ramp in JIPP T-IIU with Fast Response Zeeman Polarimeter*; Jan., 1997
NIFS-478	H. Sugama and W. Horton, *Neoclassical Electron and Ion Transport in Toroidally Rotating Plasmas*; Jan. 1997
NIFS-479	V.L. Vdovin and I.V. Kamenskij, *3D Electromagnetic Theory of ICRF Multi Port Multi Loop Antenna*; Jan. 1997
NIFS-480	W.X. Wang, M. Okamoto, N. Nakajima. S Murakami and N. Ohyabu, *Cooling Effect of Secondary Electrons in the High Temperature Divertor Operation*; Feb. 1997
NIFS-481	K. Itoh, S.-I. Itoh, H. Soltwisch and H.R. Koslowski, *Generation of Toroidal Current Sheet at Sawtooth Crash*; Feb. 1997
NIFS-482	K. Ichiguchi, *Collisionality Dependence of Mercier Stability in LHD Equilibria with Bootstrap Currents*; Feb. 1997
NIFS-483	S. Fujiwara and T. Sato, *Molecular Dynamics Simulations of Structural Formation of a Single Polymer Chain: Bond-orientational Order and Conformational Defects*; Feb. 1997
NIFS-484	T. Ohkawa, *Reduction of Turbulence by Sheared Toroidal Flow on a Flux Surface*; Feb. 1997
NIFS-485	K. Narihara, K. Toi, Y. Hamada, K. Yamauchi, K. Adachi. I. Yamada, K. N. Sato, K. Kawahata, A. Nishizawa, S. Ohdachi, K. Sato, T. Seki, T. Watari, J. Xu, A. Ejiri, S. Hirokura, K. Ida, Y. Kawasumi, M. Kojima, H. Sakakita, T. Ido, K. Kitachi, J. Koog and H. Kuramoto, *Observation of Dusts by Laser Scattering Method in theJIPPT-IIU Tokamak* Mar. 1997
NIFS-486	S. Bazdenkov, T. Sato and The Complexity Simulation Group, *Topological Transformations in Isolated Straight Magnetic Flux Tube*; Mar. 1997
NIFS-487	M. Okamoto, *Configuration Studies of LHD Plasmas;* Mar. 1997

NIFS-488 A. Fujisawa, H. Iguchi, H. Sanuki, K. Itoh, S. Lee, Y. Hamada, S. Kubo, H. Idei, R. Akiyama, K. Tanaka, T. Minami, K. Ida, S. Nishimura, S. Morita, M. Kojima, S. Hidekuma, S.-I. Itoh, C. Takahashi, N. Inoue, H. Suzuki, S. Okamura and K. Matsuoka,
Dynamic Behavior of Potential in the Plasma Core of the CHS Heliotron/Torsatron; Apr. 1997

NIFS-489 T. Ohkawa,
Pfirsch - Schlüter Diffusion with Anisotropic and Nonuniform Superthermal Ion Pressure; Apr. 1997

NIFS-490 S. Ishiguro and The Complexity Simulation Group,
Formation of Wave-front Pattern Accompanied by Current-driven Electrostatic Ion-cyclotron Instabilities; Apr. 1997

NIFS-491 A. Ejiri, K. Shinohara and K. Kawahata,
An Algorithm to Remove Fringe Jumps and its Application to Microwave Reflectometry; Apr. 1997

NIFS-492 K. Ichiguchi, N. Nakajima, M. Okamoto,
Bootstrap Current in the Large Helical Device with Unbalanced Helical Coil Currents; Apr. 1997

NIFS-493 S. Ishiguro, T. Sato, H. Takamaru and The Complexity Simulation Group,
V-shaped dc Potential Structure Caused by Current-driven Electrostatic Ion-cyclotron Instability; May 1997

NIFS-494 K. Nishimura, R. Horiuchi, T. Sato,
Tilt Stabilization by Energetic Ions Crossing Magnetic Separatrix in Field-Reversed Configuration;June 1997

NIFS-495 T. -H. Watanabe and T. Sato,
Magnetohydrodynamic Approach to the Feedback Instability; July 1997

NIFS-496 K. Itoh, T. Ohkawa, S. -I.Itoh, M. Yagi and A. Fukuyama
Suppression of Plasma Turbulence by Asymmetric Superthermal Ions; July 1997

NIFS-497 T. Takahashi, Y. Tomita, H. Momota and Nikita V. Shabrov,
Collisionless Pitch Angle Scattering of Plasma Ions at the Edge Region of an FRC; July 1997

NIFS-498 M. Tanaka, A.Yu Grosberg, V.S. Pande and T. Tanaka,
Molecular Dynamics and Structure Organization in Strongly-Coupled Chain of Charged Particles; July 1997

NIFS-499 S. Goto and S. Kida,
Direct-interaction Approximation and Reynolds-number Reversed Expansion for a Dynamical System; July 1997

NIFS-500 K. Tsuzuki, N. Inoue, A. Sagara, N. Noda, O. Motojima, T. Mochizuki, T. Hino and T.

Yamashina,
Dynamic Behavior of Hydrogen Atoms with a Boronized Wall; July 1997

NIFS-501 I. Viniar and S. Sudo,
Multibarrel Repetitive Injector with a Porous Pellet Formation Unit; July 1997

NIFS-502 V. Vdovin, T. Watari and A. Fukuyama,
An Option of ICRF Ion Heating Scenario in Large Helical Device; July 1997

NIFS-503 E. Segre and S. Kida,
Late States of Incompressible 2D Decaying Vorticity Fields; Aug. 1997

NIFS-504 S. Fujiwara and T. Sato,
Molecular Dynamics Simulation of Structural Formation of Short Polymer Chains; Aug. 1997

NIFS-505 S. Bazdenkov and T. Sato
Low-Dimensional Model of Resistive Interchange Convection in Magnetized Plasmas; Sep. 1997

NIFS-506 H. Kitauchi and S. Kida,
Intensification of Magnetic Field by Concentrate-and-Stretch of Magnetic Flux Lines; Sep. 1997

NIFS-507 R.L. Dewar,
Reduced form of MHD Lagrangian for Ballooning Modes; Sep. 1997

NIFS-508 Y.-N. Nejoh,
Dynamics of the Dust Charging on Electrostatic Waves in a Dusty Plasma with Trapped Electrons; Sep.1997

NIFS-509 E. Matsunaga, T.Yabe and M. Tajima,
Baroclinic Vortex Generation by a Comet Shoemaker-Levy 9 Impact; Sep. 1997

NIFS-510 C.C. Hegna and N. Nakajima,
On the Stability of Mercier and Ballooning Modes in Stellarator Configurations; Oct. 1997

NIFS-511 K. Orito and T. Hatori,
Rotation and Oscillation of Nonlinear Dipole Vortex in the Drift-Unstable Plasma; Oct. 1997

NIFS-512 J. Uramoto,
Clear Detection of Negative Pionlike Particles from H_2 *Gas Discharge in Magnetic Field*; Oct. 1997

NIFS-513 T. Shimozuma, M. Sato, Y. Takita, S. Ito, S. Kubo, H. Idei, K. Ohkubo, T. Watari, T.S.

Chu, K. Felch, P. Cahalan and C.M. Loring, Jr,
The First Preliminary Experiments on an 84 GHz Gyrotron with a Single-Stage Depressed Collector; Oct. 1997

NIFS-514 T. Shjmozuma, S. Morimoto, M. Sato, Y. Takita. S. Ito. S. Kubo, H. Idei, K. Ohkubo and T. Watari,
A Forced Gas-Cooled Single-Disk Window Using Silicon Nitride Composite for High Power CW Millimeter Waves; Oct. 1997

NIFS-515 K. Akaishi,
On the Solution of the Outgassing Equation for the Pump-down of an Unbaked Vacuum System; Oct. 1997

NIFS-516 *Papers Presented at the 6th H-mode Workshop (Seeon, Germany)*; Oct. 1997

NIFS-517 John L. Johnson,
The Quest for Fusion Energy; Oct. 1997

NIFS-518 J. Chen, N. Nakajima and M. Okamoto,
Shift-and-Inverse Lanczos Algorithm for Ideal MHD Stability Analysis; Nov. 1997

NIFS-519 M. Yokoyama, N. Nakajima and M. Okamoto,
Nonlinear Incompressible Poloidal Viscosity in L=2 Heliotron and Quasi-Symmetric Stellarators; Nov. 1997

NIFS-520 S. Kida and H. Miura,
Identificaiton and Analysis of Vortical Structures; Nov. 1997

NIFS-521 K. Ida, S. Nishimura, T. Minami, K. Tanaka, S. Okamura. M. Osakabe, H. Idei, S. Kubo, C. Takahashi and K. Matsuoka,
High Ion Temperature Mode in CHS Heliotron/torsatron Plasmas; Nov. 1997

NIFS-522 M. Yokoyama, N. Nakajima and M. Okamoto,
Realization and Classification of Symmetric Stellarator Configurations through Plasma Boundary Modulations: Dec. 1997

NIFS-523 H. Kitauchi,
Topological Structure of Magnetic Flux Lines Generated by Thermal Convection in a Rotating Spherical Shell; Dec. 1997

NIFS-524 T. Ohkawa,
Tunneling Electron Trap; Dec. 1997

NIFS-525 K. Itoh, S.-I. Itoh, M. Yagi, A. Fukuyama,
Solitary Radial Electric Field Structure in Tokamak Plasmas; Dec. 1997

NIFS-526 Andrey N. Lyakhov,
Alfven Instabilities in FRC Plasma; Dec. 1997